

1
2 Received Date:

3 Revised Date:

4 Accepted Date:

5 Article Type: Articles

6 Running Head: Predator effects on prey density

7 **Title: Evaluating consumptive and nonconsumptive predator effects on prey density using**
8 **field times series data**

9
10 J.A. Marino, Jr.¹⁻⁴, S.D. Peacor³, D.B. Bunnell⁵, H.A. Vanderploeg⁶, S.A. Pothoven⁷, A.K.
11 Elgin⁷, J.R. Bence³, J. Jiao³, and E.L. Ionides⁴

12
13 ¹Corresponding Author: jmarino@fsmail.bradley.edu, (309) 677-2352

14 ²Department of Biology, Bradley University, 101 Olin Hall, 1501 W. Bradley Ave., Peoria, IL
15 61625.

16 ³Department of Fisheries and Wildlife, Michigan State University, Natural Resources Building
17 480 Wilson Road, Room 13, East Lansing, Michigan 48824.

18 ⁴Department of Statistics, University of Michigan, 311 West Hall, 1085 South University, Ann
19 Arbor, MI 48109.

20 ⁵Great Lakes Science Center, U.S. Geological Survey, 1451 Green Road, Ann Arbor, MI 48105.

21 ⁶Great Lakes Environmental Research Laboratory, National Oceanic and Atmospheric
22 Administration, 4840 S. State Rd., Ann Arbor, MI 48108.

23 ⁷Lake Michigan Field Station, Great Lakes Environmental Research Laboratory, National
24 Oceanic and Atmospheric Administration, 1431 Beach St., Muskegon, MI 49441.

25
26
27 Manuscript received 7 Sep 2018; accepted 13 Nov 2018; final version received 11 Dec 2018.

28 Corresponding Editor: Caz M. Taylor

29 **Abstract**

This is the author manuscript accepted for publication and has undergone full peer review but has not been through the copyediting, typesetting, pagination and proofreading process, which may lead to differences between this version and the [Version of Record](#). Please cite this article as [doi: 10.1002/ecy.2583](https://doi.org/10.1002/ecy.2583)

This article is protected by copyright. All rights reserved

30 Determining the degree to which predation affects prey abundance in natural
31 communities constitutes a key goal of ecological research. Predators can affect prey through both
32 consumptive effects (CEs) and nonconsumptive effects (NCEs), although the contributions of
33 each mechanism to the density of prey populations remain largely hypothetical in most systems.
34 Common statistical methods applied to time series data cannot elucidate the mechanisms
35 responsible for hypothesized predator effects on prey density (e.g., differentiate CEs from
36 NCEs), nor provide parameters for predictive models. State space models (SSMs) applied to time
37 series data offer a way to meet these goals. Here, we employ SSMs to assess effects of an
38 invasive predatory zooplankter, *Bythotrephes longimanus*, on an important prey species,
39 *Daphnia mendotae*, in Lake Michigan. We fit mechanistic models in a SSM framework to
40 seasonal time series (1994-2012) using a recently developed, maximum likelihood-based
41 optimization method, iterated filtering, which can overcome challenges in ecological data (e.g.
42 nonlinearities, measurement error, and irregular sampling intervals). Our results indicate that *B.*
43 *longimanus* strongly influences *D. mendotae* dynamics, with mean annual peak densities of *B.*
44 *longimanus* observed in Lake Michigan estimated to cause a 61% reduction in *D. mendotae*
45 population growth rate and a 59% reduction in peak biomass density. Further, the observed *B.*
46 *longimanus* effect is most consistent with an NCE via reduced birth rates. The SSM approach
47 also provided estimates for key biological parameters (e.g., demographic rates) and the
48 contribution of dynamic stochasticity and measurement error. Our study therefore provides
49 evidence derived directly from survey data that the invasive zooplankter *B. longimanus* is
50 affecting zooplankton demographics and offer parameter estimates needed to inform predictive
51 models that explore the effect of *B. longimanus* under different scenarios such as climate change.

52

53 **Keywords**

54 *Daphnia mendotae*, *Bythotrephes longimanus*, nonconsumptive effects, iterated filtering,
55 predator-prey interaction, Laurentian Great Lakes

56

57 **Introduction**

58 Quantification of the effects of predators on prey abundance is important for
59 understanding ecological systems. Experiments in the field and laboratory can offer insights into
60 potential mechanisms through which predators affect prey, but translating experimental

61 measurements to field-relevant effects is challenging. For instance, in addition to consumption
62 (i.e., consumptive effects, CEs), short-term experimental and observational studies suggest that
63 nonconsumptive effects (NCEs) of predators can strongly affect prey density (Nelson et al. 2004,
64 Matassa and Trussell 2011). However, the realized importance of NCEs in natural systems has
65 recently been called into question (discussed in Kimbro et al. 2017), and the relative
66 contributions of CEs and NCEs to large-scale, long-term prey density patterns remain largely
67 unknown.

68 Existing field time series data may contain valuable information regarding the influence
69 of predators on prey abundance at field-relevant spatial and temporal scales. In effect, analyzing
70 consecutive points in time series with variable predator and prey abundances might offer
71 information about how each is affecting the other as a function of hypothesized mechanisms.
72 Challenges exist, however, to extract this information. Ecological systems are complex, e.g., due
73 to nonlinearities and stochasticity, and the collection of ecological data is subject to measurement
74 error and other constraints, such as irregular sampling intervals (Turchin and Taylor 1992,
75 Bjornstad and Grenfell 2001, Scheffer et al. 2001). Further, potentially confounding factors (e.g.,
76 seasonality, density dependence) can be difficult to disentangle from predator effects.
77 Fortunately, recent methodological advancements can confront these challenges and provide
78 insights into the contribution of different hypothesized mechanisms (Breto et al. 2009, Ionides et
79 al. 2015). Specifically, mechanistic models of population dynamics can be implemented as state
80 space models (SSMs, also known as partially observed Markov process models or hidden
81 Markov models). SSMs include both a process model representing the true population dynamics
82 and a measurement model representing the generation of the data (Newman et al. 2014). By
83 explicitly accounting for these sources of variation, SSMs allow for testing of mechanistic
84 hypotheses using time series data.

85 There are extensive time series data collected at multiple trophic levels in the Laurentian
86 Great Lakes for management purposes, and applying SSMs to these data could be useful to
87 address major questions, such as the impact of invasive species. A recent invader to the Great
88 Lakes believed to be having a major impact on the zooplankton community is the large predatory
89 cladoceran, *Bythotrephes longimanus*. For example, *Daphnia retrocurva* and *D. pulicaria*,
90 declined rapidly in Lake Michigan after the introduction of *B. longimanus* in 1986 (Lehman and
91 Caceres 1993, Barbiero and Tuchman 2004). Recent experimental and modeling research

92 suggest that *B. longimanus* could further be affecting the abundance and spatial distribution of
93 current dominant zooplankton species in the Great Lakes. Such effects are of potential
94 importance to fisheries management, because *B. longimanus* effects on zooplankton density and
95 position may reduce food availability for common prey fishes, with potential impacts on growth
96 and recruitment. In turn, effects on prey fishes may affect key fisheries, such as Chinook salmon,
97 that depend on those planktivores (Jacobs et al. 2013, Bunnell et al. 2015).

98 Simulation and statistical modeling as well as experimental research suggest that *B.*
99 *longimanus* influences the composition and density of mesozooplankton through both CEs and
100 NCEs. *B. longimanus* is known to prey on zooplankton (Vanderploeg et al. 1993) and
101 bioenergetics models indicate planktivory by *B. longimanus* can be substantial (Bunnell et al.
102 2011). NCEs are hypothesized to occur when zooplankton prey perceive *B. longimanus* through
103 chemical cues and adopt anti-predatory behavior in response to higher *B. longimanus* densities
104 by migrating to lower depths (Pangle and Peacor 2006, Bourdeau et al. 2011), which reduces
105 predation risk but at the cost of reduced growth rate and reproduction due to colder water at
106 lower depths (Pangle et al. 2007). Previous research has estimated CEs and NCEs on
107 zooplankton population growth rates (Pangle et al. 2007). Consumptive rates measured in the
108 laboratory can be used to estimate consumptive rates the field. NCEs can be estimated from
109 known temperature dependent effects on zooplankton birth rate and field measurements of the
110 effect of *B. longimanus* on zooplankton position (and hence the temperatures that those
111 zooplankton experience). Results yield an estimate of the relative magnitude of NCEs and CEs
112 on demographic rates, and thus serve to highlight potential influence of NCEs through
113 simulations. However, this approach cannot determine if *B. longimanus* is actually affecting the
114 density of zooplankton in the field; e.g., there could be feedback mechanisms or indirect effects
115 which would offset the predicted negative effects. Therefore, while we can predict mechanisms
116 by which *B. longimanus* affects zooplankton population growth rate (e.g., as in Pangle et al.
117 2007), evaluating the extent to which *B. longimanus* affects zooplankton prey density in the field
118 is a major challenge and could benefit from methods that allow for inference directly from field
119 density data. This problem is not unique to the Great Lakes zooplankton system, as we are aware
120 of many studies that examine the influence of NCEs on prey demographic rates in the field (e.g.,
121 Peckarsky et al. 2008, Kimbro et al. 2017), but few that examine if NCEs are affecting prey
122 density directly from prey density patterns.

123 Herein our approach is to use SSMs to test the hypothesis that *B. longimanus* influences
124 the density of an important zooplankton species, *Daphnia mendotae*, in the field through CEs
125 and NCEs. We focus on *D. mendotae* because it composes a relatively high biomass among
126 cladocerans in the community (Vanderploeg et al. 2012) and is consumed by planktivorous
127 fishes (Bunnell et al. 2015). Multiple population models of *D. mendotae*, with different
128 functional dependence on its predator, *B. longimanus*, were implemented as SSMs and fit to time
129 series data via a recently developed, maximum likelihood-based optimization method, iterated
130 filtering. Iterated filtering can fit nonlinear, non-Gaussian, non-stationary SSMs to data and
131 handle complexities associated with ecological data like irregular sampling intervals (Ionides et
132 al. 2006, 2015). Such complexities are intrinsic to complex ecological systems and field survey
133 data, including those available for the Great Lakes. Iterated filtering algorithms are distinguished
134 from other state space model methodology by providing statistically efficient, simulation-based,
135 maximum likelihood inference for general nonlinear state space models (Ionides et al., 2015).
136 Our approach should allow us to estimate key biological rates (e.g., birth and death rates) and the
137 magnitude of predator effects, as well as the contribution of stochasticity to dynamics and the
138 influence of measurement error on variation in the data, which are important to account for in
139 order to successfully address our hypothesis.

140 We had two goals: 1) Evaluate if, and to what extent, *B. longimanus* affects *D. mendotae*
141 density and, if so, whether such effects are more consistent with CEs or NCEs. 2) Estimate key
142 parameters (e.g., birth and predation rates) needed to model this system, which will be valuable
143 in the future to predict dynamics under different scenarios (e.g., climate change effects).

145 **Methods**

146 *Data description*

147 *D. mendotae* and *B. longimanus* biomass density data were collected as part of a long-
148 term survey of Lake Michigan zooplankton by the NOAA Great Lakes Environmental Research
149 Laboratory (GLERL) at an offshore site near Muskegon, MI (depth = 110 m; 43° 11.99', 086°
150 34.19'; located about 20 km offshore). The survey quantified the biomass density of crustacean
151 zooplankton 7-16 times per year across 16 years (1994-2003, 2007-2012) using whole water
152 column vertical net tows (details on sampling and biomass density calculations presented in
153 Vanderploeg et al. 2012).

154

155 *General process model of population dynamics*

156 The process model represents dynamics of *D. mendotae* using a stochastic, seasonally-
157 forced variant of a logistic population growth model. The state variable is *D. mendotae* biomass
158 density, V (i.e., the prey zooplankton), and dynamics are represented by the following stochastic
159 differential equation with respect to time, t :

$$dV = \left(V \beta(t) \left(1 - \frac{V}{\kappa} \right) (1 - \eta g(P)) - f(V)P - \mu V \right) dt + V \epsilon dW + \rho(t) \quad (1),$$

160 where $\beta(t)$ is a function representing prey birth and/or somatic growth rate at low population
161 size, and κ is a prey density dependence term (here affecting prey birth/somatic growth rate). The
162 term $\eta g(P)$ determines the nonconsumptive effect of *B. longimanus* on *D. mendotae* via a
163 proportional reduction in birth rate, with P representing *B. longimanus* biomass density treated as
164 a covariate (not dynamically modeled). The functional response $f(V)$ determines the
165 consumptive effect, and μ is the background mortality rate of *D. mendotae* not due to
166 consumption by *B. longimanus*. The NCE and CE of *B. longimanus* are described in more detail
167 below (see: *Consumptive and nonconsumptive predator effects*). The $V \epsilon dW$ term allows for
168 random variation to occur in *D. mendotae* dynamics (i.e., process error), which can occur due to
169 factors influencing growth rates not specified in the model, such as variation in weather. The
170 standard deviation ϵ scales the process error dW , and this process variation is driven by
171 Brownian motion:

$$dW \sim \text{Normal} (\text{mean} = 0, \text{sd} = \sqrt{dt}) \quad (2),$$

172

173 which is a common way to represent stochasticity in dynamic population models (Panik 2017).
174 The term $\rho(t)$ represents the initiation of *D. mendotae* dynamics each year via emergence from
175 resting eggs. Briefly, $\rho(t)$ is modeled as a pulse that only contributed to the population on the
176 first day of each year's dynamics and is equal to zero on other days (see *Initiation of dynamics*
177 *each year* for more detail).

178

179 *Seasonality in prey birth rate*

180 We modeled seasonality in *D. mendotae* birth rate given known strong seasonality in
181 abundance due to factors such as temperature, light levels, and resources that affect birth rate
182 using the equation:

$$\beta(t) = \exp \left\{ \sum_{i=1}^{N_s} \lambda_i s_i(t) \right\} \quad (3),$$

183 where $\{s_i(t), i = 1, \dots, N_s\}$ is a periodic cubic B-spline basis with 4 bases ($N_s = 4$), a degree of 3,
184 and a period of 1 year; $\{\lambda_i, i = 1, \dots, N_s\}$ are parameters that specify the seasonality of the birth
185 rate.

186 $\beta(t)$ is intended to capture *D. mendotae* seasonality using a function allowing enough
187 flexibility to capture dynamics while avoiding overly complicating the model (i.e., adding
188 unnecessary parameters). A periodic b-spline with $N_s > 3$ provides a more flexible representation
189 of seasonal forcing compared to a sinusoidal, which has been used to represent seasonality in
190 biological parameters. Tests that we performed using $N_s > 4$ suggested that additional parameters
191 result in worse model performance based the Akaike Information Criterion (AIC), a measure of
192 model quality, than $N_s = 4$. Eq. 3 therefore provides a reasonable representation of the
193 seasonality in *D. mendotae* dynamics.

194

195 *Consumptive and nonconsumptive predator effects*

196 For the CE, we used a Type I functional response, $f(V) = \alpha V$, where α is *B. longimanus*
197 attack rate on *D. mendotae*, as an approximately linear response is expected at the *D. mendotae*
198 densities found in the survey according to laboratory predation experiments (Pangle and Peacor,
199 unpublished data). We also evaluated an alternative version of the model with a Type II
200 functional response (see: *Evaluation of Type II Functional Response*).

201 Nonconsumptive effects of *B. longimanus* on *D. mendotae* birth rate are represented by
202 the proportion reduction in birth rate ($\eta g(P)$) according to the equation for $g(P)$:

$$g(P) = 7.601 + \ln(P + 0.0005) \quad (4)$$

203 We used a logarithmic function based on the log-linear relationship of the behavioral (i.e.
204 vertical migration) response of *D. mendotae* to *B. longimanus* density (e.g., Bourdeau et al.
205 2015) that leads to an expected reduction in birth rate due to the colder temperatures in deeper
206 water. A correction term (0.0005) was used to account for zero observations equivalent to ½ the
207 smallest observation of *B. longimanus*. The equation for $g(P)$ includes the negative natural log of

208 the correction term ($-\ln(0.0005) = 7.601$) to be consistent with a reduction in birth rate (i.e.,
209 to eliminate the potential for a positive effect of *B. longimanus* biomass density on population
210 growth at low *B. longimanus* densities).

211 The effects of *B. longimanus* were modeled as forcing functions in which the potential
212 dynamic feedbacks to *B. longimanus* density are not included in the model for two reasons. First,
213 there are likely other factors that affect *B. longimanus* density, including other prey items (e.g.,
214 copepods, *Bosmina longirostris*, and other *B. longimanus*), predation by fish, and physical
215 factors (e.g., variable water currents, temperature) (Keeler et al. 2015). Second, treating *B.*
216 *longimanus* as a state variable would require a substantial increase in the complexity of the
217 model due to the potentially large number of additional parameters needed to model *B.*
218 *longimanus* dynamics. Adding such additional complexity would substantially increase the
219 challenge of fitting the model, due to having to estimate multiple additional parameters with a
220 limited number of available data points ($n = 134$).

221 To reduce the influence of measurement error on estimates for *B. longimanus* (note: the
222 measurement error model in Eq. 7 and 8 below applies only for the *D. mendotae* state variable),
223 which could influence our estimates for predator effects, smoothing was performed by
224 calculating a moving average for *B. longimanus*, *P*. We used a 45-day window for the moving
225 average, which we expected should minimize information lost while reducing the influence of
226 measurement error. This window was chosen because the mean gap between observations
227 (excluding gaps between years) was 21 days, so that the value for the moving average on each
228 day was typically influenced by 2-3 observations. We expected that a shorter window for the
229 moving average would be insufficient given the mean time gap between observations, while a
230 longer window could smooth over too much potentially informative variation in *B. longimanus*
231 given the typical generation time of *B. longimanus* (7-15 days, Kim and Yan 2010). Further, tests
232 using a longer (e.g., 59-day) and shorter (e.g., 7-day) window for the moving average resulted in
233 worse fits based on maximum likelihood estimates than the 45-day window. Similar tests
234 comparing different durations have been used in other systems to establish the appropriate
235 window for assessing impacts of other important covariates, such as climatic factors (van de Pol
236 et al. 2016). Further, tests we performed using alternative methods of interpolation and
237 smoothing (i.e., $\ln(+0.0005)$ transformation of *B. longimanus* data prior to calculation of a

238 moving average or using a moving 45-day median) did not offer improvement in model
239 performance based on AIC, and did not substantially affect our results.

240 The calculation of the moving average for *B. longimanus* biomass density involved two
241 steps. First, daily estimates of biomass density were interpolated linearly between observations
242 for gaps between observations, with the exception of the gap between the last observation each
243 year and the first observation of the subsequent year. Interpolation is necessary, as the model
244 represents continuous-time dynamics, so that a value for each covariate is required at each time
245 step. The gap between years was treated differently because data were rarely collected during
246 winter and early spring, and *B. longimanus* is typically absent from the water column at that
247 time, while the population is maintained as resting eggs. We therefore assumed that *B.*
248 *longimanus* is absent for the first 50 days each year (i.e., we set *B. longimanus* biomass density
249 to 0 for those days), prior to the interpolation.

250 Second, these interpolated values (P_{int}) were then used to calculate a 45-day geometric
251 mean (P). The correction term (0.0005, as for Eq. 4) was used to calculate the geometric mean to
252 account for the presence of 0s in the *B. longimanus* data (otherwise the mean would be 0 for any
253 time points with a 0 in the 45-day moving average window). The P covariate for each time (t)
254 was thus:

$$P(t) = \left(\prod_{i=1}^{45} P_{int}(t - 23 + i) + 0.0005 \right)^{1/45} - 0.0005 \quad (5)$$

255
256 *Initiation of dynamics each year*

257 Because *D. mendotae* are effectively absent from the water column in winter, we allowed
258 the population in the water column to go extinct each winter and be reseeded via a pulse ($\rho(t)$)
259 representing the emergence from resting eggs each spring occurring 7 days prior to the earliest
260 observation of *D. mendotae* in the data. The size of the pulse is not well understood. In fact, it is
261 plausible that the abundance of neonates emerging from resting eggs is not strongly dependent
262 on the previous year's density given that resting eggs can survive for multiple years (Caceres
263 1998) and strong variation occurs in physical processes that promote hatching (Kerfoot et al.
264 2004). We therefore assumed the size of the pulse was random and log-normally distributed:

$$\ln(\rho(t)) \sim \text{Normal}(\phi, \psi) \quad (6)$$

265 ϕ and ψ represent the mean and standard deviation of the natural log of the pulse, respectively.

266

267 *Measurement model*

268 A measurement model is used to describe how observations (i.e., the data, which are
269 subject to measurement error) were generated from the prey biomass state variable, which
270 represents the true biomass density; therefore, the observed data are treated as drawn from a
271 distribution around the true state of the system. Measurement error in this sense is general,
272 including any differences between samples collected on different days not attributable to changes
273 in the true biomass density (e.g., due to differences between two net tows due to small-scale
274 spatial variation or potential short-term fluctuations due to water currents or responses to
275 variation in light levels that could affect individual measurements). We used a left-censored
276 normal (Normal_{l-cens.}) distribution (e.g., Martinez-Bakker et al. 2015, in which the probability of
277 a zero value is treated as a point mass equal to the censored left tail of the normal distribution).
278 Two parameters (σ_a and σ_b) are specified so that the variance (σ^2) scales quadratically with
279 population size:

$$V_{obs(t)} \sim \text{Normal}_{l-cens.}(V_t, \sigma) \quad (7)$$

$$\sigma \sim \sqrt{\sigma_a^2 V_{(t)} + \sigma_b^2 V_{(t)}^2} \quad (8)$$

280 We used a left-censored distribution to account for zero observations in the data and because
281 negative observations cannot occur. The left-censored model assumes that the observed biomass
282 density at any time point is normally distributed around the true biomass density, with a standard
283 deviation that scales with population size according to Eq. 8, except the left-censored model does
284 not allow observations of negative biomass density.

285

286 *Model modifications to assess dynamic drivers*

287 To examine the influence of *B. longimanus*, we fit four versions of the model to the data:
288 model a) a null model (i.e., excluding any *B. longimanus* effect by fixing α and η at 0); model b)
289 a model including only the NCE (i.e., fixing α at 0); model c) a model including only the CE
290 (i.e., fixing η at 0); and model d) a model including both the CE and NCE.

291

292 *Benchmark Statistical Models*

293 A reasonable mechanistic model should perform better than a simple, non-mechanistic
294 benchmark model (King et al. 2008). We therefore compared our mechanistic models to two
295 straightforward benchmark models. First, we used a model assuming observed *D. mendotae*
296 biomass density is independently and identically distributed around a seasonal (monthly) average
297 (model e):

$$Vobs_{(t)} \sim \text{Normal}_{l-cens.}(D_m, \sigma) \quad (9)$$

$$\sigma \sim \sqrt{\sigma_a^2 D_m + \sigma_b^2 D_m^2} \quad (10)$$

298 D_m represents mean biomass densities for each month that observations were made, and
299 observations are assumed to follow a left-censored normal distribution, as for models a-d
300 (although model e does not differentiate between measurement and process error). Second, we fit
301 an AR (2) autoregressive model with measurement error to our time series (model f), in which
302 the observed *D. mendotae* biomass density depends linearly on the previous two observations.
303 We used the same measurement model (Eq. 7 and 8) for model f as for models a-d, so as to allow
304 for zero but no negative observations.

305

306 *Model fitting*

307 Analyses were implemented using the pomp package in R v.3.3.3 (R Core Team 2018),
308 and annotated code is included in Appendix S1. SSMs (including all models except model e,
309 which was fit using the R optim function) were fit to time series data using iterated filtering via
310 the mif2 algorithm, which is a recently developed algorithm for estimating model parameters via
311 maximum likelihood estimation that offers substantial improvement over other SSM fitting
312 methods (Ionides et al. 2015, King et al. 2016). For each model fit using iterated filtering, we
313 performed 100 runs in which a search through parameter space was initiated using a random set
314 of starting values for each parameter. Starting values were generated from a uniform distribution
315 bounded by broad plausible values for each parameter. The fit of different models was compared
316 based on the Akaike Information Criterion (AIC) calculated using the maximum likelihood
317 estimate, which provides a measure of model performance that weighs both model complexity
318 based on the number of parameters and fit based on the likelihood (Akaike 1974). A difference
319 of 2 AIC units indicates a substantial improvement in model performance (Burnham and
320 Anderson 2002).

321

322 *Magnitude of B. longimanus effect*

323 To quantify effects of *B. longimanus* on *D. mendotae* biomass density, we used
324 simulations from the fitted model (model b, the best model based on AIC, see results). We
325 compared biomass densities of *D. mendotae* in 10,000 simulated 1-year data sets including or
326 excluding the effect of *B. longimanus* by setting η to the maximum likelihood estimated value or
327 0, while all other parameters were fixed at their maximum likelihood estimated values. The
328 simulations used an across-year seasonal mean of smoothed *B. longimanus* biomass density for
329 predator biomass density. We note that these simulations necessarily do not reflect the full range
330 of actual variation in the system (e.g., due to uncertainty in parameter estimates) but provide a
331 straightforward way to quantify and visualize reductions in *D. mendotae* biomass density caused
332 by estimated effects of *B. longimanus*.

333

334 *Parameter estimates and confidence intervals*

335 To gain further insight into the influence of *B. longimanus* and density dependence on
336 dynamics, we developed confidence intervals for the model estimates of the NCE (η) and density
337 dependence (κ) parameters using profile likelihood (Hilborn and Mangel 1997). In profile
338 likelihood, the likelihood is maximized and all other parameters are estimated across a fixed
339 plausible range of values of the focal parameter (i.e., η or κ in our case). The result is a profile
340 that shows how the maximum likelihood changes depending on that focal parameter value. The
341 95% confidence intervals are determined as the range of parameter values for which the log-
342 likelihood is within 1.92 units of the maximum log-likelihood (Hilborn and Mangel 1997).

343

344 *Evaluation of potential influence of seasonality*

345 We were concerned that seasonality may confound results for two reasons. First, because
346 *B. longimanus* and *D. mendotae* densities vary seasonally, we were concerned that a detected
347 effect of *B. longimanus* was actually due to other seasonal factors that covary with *B.*
348 *longimanus* but are not included in the model. Second, the NCE in the model is part of an
349 expression that includes a seasonality term ($\beta(t)$), but the CE is part of an expression without
350 seasonality, so that a difference in the influence of the NCE and CE could potential be influenced

351 by the difference in their relationship with seasonality in the model. We therefore performed
352 three additional analyses to examine the influence of seasonality.

353 First, we wanted to compare the performance of our model using *B. longimanus* as the
354 predator to another species that we would not expect to affect *D. mendotae*. We therefore
355 examined the fit of the best performing model (model b, see Results) substituting the biomass
356 density data for another species, *Limnocalanus macrurus*, as an alternative predator instead of *B.*
357 *longimanus* (model g). As *L. macrurus* mostly occurs in the hypolimnion and would have limited
358 spatial overlap with *D. mendotae*, we would not expect it to have a detectable effect on *D.*
359 *mendotae*. However, *L. macrurus* also exhibits strong seasonality in its dynamics (Vanderploeg
360 et al. 2012), so that treating it in the same manner as *B. longimanus* (i.e., as a predator) in the
361 model provides a useful comparison to evaluate if seasonality itself could be responsible for any
362 detected predatory effect of *B. longimanus*. A test using *L. macrurus* thereby directly addresses
363 whether the methods would have identified a spurious relationship for this particular species.

364 Second, we calculated a *B. longimanus* biomass density anomaly (deviations from the
365 average seasonal trend across years, i.e., with the seasonal trend removed) and compared how the
366 model performed when using the anomaly compared to the null model (model h; see Appendix
367 S1 for details). Because the anomaly excluded the seasonal trend, we would expect that including
368 the anomaly should substantially improve the model AIC over a null model if there is an effect
369 of *B. longimanus* distinct from a seasonal effect.

370 Third, we examined two additional models to address alternative hypotheses for how
371 seasonality influences *D. mendotae* dynamics: model i) a modified version of the null model
372 (model a) that includes seasonal background mortality, μ ; and model j) a modified version of the
373 model with only CEs (model c) that allows seasonal change in *B. longimanus* attack rate, α . In
374 both models, each parameter was allowed to vary seasonally using periodic b-splines in the same
375 manner as birth rate (β) (Eq. 3). We performed these analyses to ensure that our finding of an
376 NCE of *B. longimanus* (see Results) could not be explained by seasonality in background
377 mortality or *B. longimanus* consumption.

378 *Evaluation of Type II Functional Response*

379 In addition, to ensure that our results did not depend on the choice of functional response
380 used in our model, we modified model c to include a Type II functional response for $f(V)$:

$$f(V) = \frac{\alpha V}{1 + \alpha h V} \quad (11),$$

381 where h represents *B. longimanus* handling time for *D. mendotae* (model k).

382

383 **Results**

384 The mechanistic SSMs performed substantially better than the benchmark models based
385 on AIC (Table 1).

386 The models including the NCE of *B. longimanus* on *D. mendotae* outperformed the
387 alternative models based on a comparison of AIC values. In contrast, including the CE did not
388 improve the model performance either in the absence or inclusion of the NCE. Only the model
389 with both the CE and NCE was within 2 AIC units of the best fit model that included the NCE
390 but not the CE (model b). Because the former model included an additional parameter and
391 offered no improvement over the latter model, we moved forward with model b as the best
392 model.

393 To visualize the fit of the best model, we generated 10,000 simulated data sets (including
394 the contribution of both process and measurement errors) from the fitted model using the
395 parameter values at the maximum likelihood estimate (Table 2). Quantiles of the resulting
396 simulations are shown to represent the median and 95% simulation intervals (Fig. 1). The clear
397 seasonality of the simulation median suggests strong, predictable seasonality of *D. mendotae*
398 dynamics. In contrast, differences between years are subtler and less predictable. The relatively
399 broad 95% simulation intervals reflect relatively high levels of variation among simulations,
400 attributable to dynamic stochasticity and measurement error. All but four observations fall within
401 the simulation intervals, with the two most notable exceptions being the especially high peaks in
402 the *D. mendotae* data in 2011 and 2012. In these years, *B. longimanus* had especially high
403 density earlier in the season, for which the model would predict lower *D. mendotae* densities
404 than observed those years.

405 The maximum-likelihood parameter estimates indicate *B. longimanus* can have a
406 profound influence on *D. mendotae* density. Based on the fitted model estimate for η , *D.*
407 *mendotae* birth rates are reduced by 61% at the mean peak *B. longimanus* across years (Fig. 2a).
408 Simulations from the model generated using the maximum-likelihood estimate compared to
409 simulations generated using the same values for other parameters but excluding the effect of *B.*

410 *longimanus* (i.e., setting η equal to 0) suggests that the nonconsumptive effect on population
411 growth rate results in as large as a 59% reduction in *D. mendotae* biomass density (difference
412 between height of peaks in Fig. 2b). The likelihood profile for η reveals our level of confidence
413 in our parameter estimate (Fig. 3a, showing 95% confidence intervals). Using the lowest and
414 highest value of η (at confidence interval bounds), at the mean annual peak of *B. longimanus*,
415 the NCE ranges from a 28% to 82% reduction in growth rate.

416 The fitted SSM also provides estimates for the contribution of seasonality to *D. mendotae*
417 dynamics. The fitted seasonal function for *D. mendotae* birth rates suggests a peak on Julian day
418 229 (August 16) in late summer. In the presence of *B. longimanus* at its mean biomass density,
419 the peak both shifts in timing (10 days earlier to Julian day 219) and is reduced due to the NCE
420 (Fig. 2a).

421 Density dependence also influences *D. mendotae* dynamics, based on parameter estimate
422 and its confidence interval (Table 2, Fig. 3b). The parameter estimate for κ ($33 \text{ mg} \times \text{m}^{-3}$) was
423 within the range of observed *D. mendotae* biomass density ($0\text{-}74 \text{ mg} \times \text{m}^{-3}$), with 6 observations
424 of *D. mendotae* biomass density exceeding the estimated value for κ , suggesting that high
425 conspecific densities may almost entirely suppress positive *D. mendotae* growth under realized
426 conditions in Lake Michigan.

427 Other parameter estimates provide insights into the contribution of measurement error
428 and process stochasticity. Based on Eq. 7 and 8, the estimates for σ_a and σ_b indicate that the
429 standard deviation of observed biomass at mean *D. mendotae* biomass was approximately 40%
430 of mean, indicating a substantial impact of measurement error. The estimate for the standard
431 deviation of *D. mendotae* growth rate (ϵ) is also large (126% of the maximum seasonal growth
432 rate when at low population size, $\beta(t)$), suggesting the importance of process stochasticity as
433 well. Both process stochasticity and measurement error thus contribute to the high levels of
434 variation in the data (Fig. 1).

435

436 *Evaluation of potential influence of seasonality*

437 The three tests indicate that the result that *B. longimanus* affected *D. mendotae* through
438 an NCE was not confounded by seasonality. First, using *L. macrurus* biomass density as the
439 predator (model g) had the opposite effect than using *B. longimanus* as it performed worse than
440 the model with no predator effect (model a) based on AIC (Table 1). Second, using the *B.*

441 *longimanus* anomaly (model h) substantially improved the model fit compared to the model
442 without effects of *B. longimanus*, despite the removal of the across-year seasonal trend, thereby
443 providing further evidence for an effect of *B. longimanus* independent of seasonal factors. If the
444 observed effect of *B. longimanus* was due to other seasonal confounding factors, no
445 improvement would be expected by only using the anomaly. Notably, however, the model using
446 the anomaly did not perform as well as the model using the actual *B. longimanus* biomass
447 density data (model b), suggesting both anomalous and seasonal variation in *B. longimanus*
448 contribute to *D. mendotae* dynamics. Third, if our detection of the NCE was caused by a
449 confounding factor associated with the seasonal nature of the birth rate term, we would expect
450 that adding seasonality to the mortality or attack rate (models i or j) would have a similar
451 influence to including the NCE. However, models i and j performed substantially worse than
452 model b (Table 1), supporting the importance of the NCE.

453 *Evaluation of Type II Functional Response*

454 Finally, tests using an alternative (Type II) functional response (model k) revealed that
455 our findings were not sensitive to the assumed functional response for the CE.

456

457 **Discussion**

458 Our analysis provides evidence that *B. longimanus* has strong negative effects on *D.*
459 *mendotae* population growth rate and density in offshore Lake Michigan and supports the
460 hypothesis that an NCE is the underlying mechanism. Further, our analysis quantifies key
461 demographic rates for *D. mendotae*, including birth and death rates, which can be used in models
462 that forecast the effects of future changes, such as climate change or changes in nutrient
463 concentrations, with implications for overall Lake Michigan food web dynamics and fisheries.
464 Our results demonstrate the utility of developing SSMs and fitting them to field time series data
465 to assess mechanisms by which predators affect prey, despite the challenges intrinsic to
466 ecological systems and data.

467 Our findings provide evidence of and, for the first time to our knowledge, quantify NCEs
468 derived from field-based time series data in a mechanistic framework. The observed negative
469 effect of *B. longimanus* on *D. mendotae* population growth rate resulted from an NCE in which
470 *B. longimanus* reduced *D. mendotae* birth/somatic growth rates. Of the mechanistic models
471 compared, the model including NCEs but not CEs provided the best fit relative to the number of

472 parameters based on AIC, and greatly reduced AIC relative to the addition of CEs alone.
473 Whereas, NCEs have received considerable attention, most studies have been performed in a
474 laboratory setting, mesocosms, and enclosures. Further, whereas there is an increasing number of
475 studies performed in the field, very few studies examine the influence on density based on field
476 data (Sheriff et al. in review). For example, previous studies evaluating NCEs of *B. longimanus*
477 on *D. mendotae* (Pangle et al. 2007, Bourdeau et al. 2013) combined laboratory studies that
478 elucidate the behavioral response of *D. mendotae* to *B. longimanus* with field survey data of *D.*
479 *mendotae* vertical position at different densities of *B. longimanus*. Using temperature-dependent
480 growth models, these studies predicted a large reduction in fitness of *D. mendotae* due to lower
481 temperatures experienced at the lower depths occupied as a result of the anti-predator response to
482 *B. longimanus*. Similarly, other studies that have examined NCEs in the field, have, for example,
483 combined knowledge of predation rates and induced changes in prey behavior to explain
484 hypothesized nonconsumptive effects on spatial variation in prey abundance (e.g., wolf
485 avoidance by elk in Yellowstone, Creel et al. 2005, shark avoidance by marine vertebrates,
486 Heithaus et al. 2009). Our approach to documenting NCEs from field data here is qualitatively
487 different, in that evidence was derived directly from changes in density of prey in relation to
488 changes in predator density, linked through mechanistic models.

489 We examined the time series data, and the model fits, to interpret why the inclusion of the
490 NCE in the model leads to a large improvement in model performance, but adding the CE does
491 not. Importantly, because *D. mendotae* birth rates peak earlier than peak *B. longimanus* density,
492 the NCE exerts its major influence earlier than when CE effects are maximized. Thus, the model
493 estimates the strongest *B. longimanus* effects in years when *B. longimanus* biomass density
494 reaches high levels early, when *D. mendotae* birth rates would otherwise be high. This contrasts
495 with a CE, which as modeled in Eq. 1 increases mortality the same amount whenever *B.*
496 *longimanus* density is high, regardless of time of year. This aspect of the NCE is seen in the
497 temporal patterns in the data. For example, we can calculate a 45-day moving average of *D.*
498 *mendotae* biomass density ($D_{avg}(t)$) as we did for *B. longimanus* (Eq. 5, using a modified
499 correction factor equal to one half the lowest observation for *D. mendotae*) and then estimate the
500 rate of *D. mendotae* population change (r_{est}) early in the growing season (days 175-225) each
501 year:

$$r_{est} = \ln(D_{avg}(225)/D_{avg}(175)) \quad (12)$$

502 Consistent with the NCE detected by the model, the rate of *D. mendotae* population change
503 between days 175 and 225 was negatively related to *B. longimanus* biomass density during that
504 same period (geometric mean of smoothed *B. longimanus* biomass density + 0.0005 over days
505 175-225) in the same year (Fig. 4). While it is impossible to entirely rule out that consumption of
506 *D. mendotae* by *B. longimanus* partly contributed to this pattern, model performance including
507 only the CE was substantially poorer than the NCE model, even when we relaxed the assumption
508 of a fixed attack rate by allowing it to vary seasonally (model j). The NCE therefore provides the
509 most parsimonious explanation.

510 The large magnitude of the estimated effects of *B. longimanus* on *D. mendotae* biomass
511 density here likely have important consequences for the Lake Michigan food web and are also
512 likely relevant for the other four Great Lakes where *B. longimanus* and *D. mendotae* co-occur.
513 For example, planktivorous fishes in Lakes Michigan and Huron have undergone declines in
514 biomass since the 1990s, and these fish are key prey to Chinook salmon *Oncorhynchus*
515 *tshawytscha* and lake trout *Salvelinus namaycush* that are the foundation of a multi-million dollar
516 recreational fishery (Bunnell et al. 2014). Given that survival of larval planktivorous fish in the
517 first few weeks of life can depend on overlap with zooplankton prey (Beaugrand et al. 2003),
518 understanding the mechanisms that regulate zooplankton densities is critical to improved
519 understanding and prediction of planktivorous fish recruitment. Our model estimates of *D.*
520 *mendotae* vital rates can also be applied to future decision-support tools that explore how future
521 climate or nutrient concentrations (perhaps modeled through modifications to carrying capacity,
522 κ) would affect the dynamics of *D. mendotae*, the most important herbivorous cladoceran in
523 terms of biomass (Vanderploeg et al. 2012).

524 Perhaps surprisingly, including CEs of *B. longimanus* did not substantially improve
525 model fit either alone or in combination with nonconsumptive effects. Experiments demonstrate
526 that *B. longimanus* predation rates on *D. mendotae* can be high (Vanderploeg et al. 1993, Pangle
527 and Peacor 2009), and thus one might expect high CEs in the field. Migration in response to *B.*
528 *longimanus* chemical cues (Pangle et al 2006) could be expected to reduce *B. longimanus*
529 consumption, although some studies still show spatial overlap between *B. longimanus* and *D.*
530 *mendotae* for at least a portion of the *D. mendotae* population (Bourdeau et al. 2015, Nowicki et
531 al. 2017). Nevertheless, we found little evidence for a substantial effect of consumption here.
532 One possible explanation is that our model for *B. longimanus* predation (i.e., Type I functional

533 response) may exclude key biological realism; for example, explicitly incorporating potentially
534 critical covariates that can influence predation rates, such as light levels (Pangle and Peacor
535 2009) and temperature (Yurista et al. 2010), could be explored in future models and may allow
536 for improved estimation of CEs.

537 Distinguishing between CEs and NCEs from observational data, as we have done here,
538 depends on assumed functional relationships. However, an advantage of SSMs is that
539 assumptions are made explicit in the equations and can be further tested in future work or
540 compared to experimental findings. For instance, a key difference between how CEs and NCEs
541 are modeled here is that we assume that the NCE affects birth rate or somatic growth rate, which
542 we model with a seasonal functional form, given known seasonal effects of temperature and food
543 resources on birth rate. Thus, the per capita NCE of *B. longimanus*, ($\eta g(P)$), varies seasonally in
544 magnitude in proportion to *D. mendotae* birth rate as modeled, unlike the CE, which contributes
545 additively to mortality (i.e., proportional to *B. longimanus*). These different functional forms
546 thereby allowed us to at least partially differentiate between a CE and an NCE. Evidence for the
547 latter was then strengthened by additional tests under different assumptions (e.g., allowing
548 seasonal variation in consumptive effects in model j) and comparisons to prior work that also
549 suggest the importance of NCEs (e.g., Pangle and Peacor 2006).

550 Fish predation is also an important consideration for *D. mendotae*-*B. longimanus*
551 dynamics, although we do not expect fish effects to confound our results. In fact, *B. longimanus*
552 is susceptible to fish predation from alewife (*Alosa pseudoharengus*) and other species (Bunnell
553 et al. 2015), and so more *B. longimanus* may be associated with overall lower fish predation on
554 zooplankton. That we saw declines in *D. mendotae* biomass density associated with higher *B.*
555 *longimanus* despite potentially reduced risk from planktivorous fish at these times thus provides
556 further support that effects of *B. longimanus* are important for *D. mendotae* dynamics, and that
557 *B. longimanus* may be an important competitor with fish for zooplankton prey.

558 Another concern with analyses of field data relevant to our study is disentangling the
559 influence of seasonality from other dynamical drivers, such as the effects of *B. longimanus*. We
560 chose a flexible approach to incorporate seasonality in the system (periodic b-splines), and the
561 additional tests we performed (i.e., using *L. macrurus*, the anomaly, or allowing other terms to
562 vary seasonally) offered further support that other seasonal factors were not responsible for the
563 observed effect of *B. longimanus*. Similar rigorous tests should be a broadly useful approach to

564 disentangle seasonality from other drivers in many systems using SSMS. By using these tests, our
565 approach here was conservative in attempting to rule out a confounding effect of seasonality; in
566 fact, beyond the NCE we detected, it is plausible that *B. longimanus* effects on *D. mendotae* may
567 also actually contribute to the estimated effect of seasonal forcing. We may therefore be
568 underestimating a CE or an NCE if they are attributed to and therefore subsumed by the seasonal
569 model terms; explicitly considering some seasonal factors (e.g., temperature, resources) in future
570 may allow better resolution of these effects. In particular, future models including additional data
571 for spatial variation in *D. mendotae*, *B. longimanus*, resources, and temperature may allow better
572 resolution of the relative contribution of seasonality, CEs, and NCEs, as water column structure
573 likely plays an important role in mediating *B. longimanus* effects.

574 Our approach was also useful to quantify the influence of other drivers of *D. mendotae*
575 dynamics, including seasonality and density dependence. Model results reflect how *D. mendotae*
576 birth rates and biomass density change with Julian day (Fig. 3), likely due to seasonal variation
577 in temperature, food resources, water column structure, or other factors. Similarly, the estimated
578 density dependence term (κ) and its confidence interval indicate that *D. mendotae* population
579 growth is substantially density dependent under field conditions in Lake Michigan, potentially
580 due to competition for food resources. Further, estimates of density dependence will be vital for
581 predicting impacts of ongoing changes in the lower food web (Fahnenstiel et al. 2010). Our
582 findings thus motivate future work to investigate the underlying mechanisms driving seasonality
583 and density dependence and implications to other parts of the food web.

584 Our findings also provide estimates for the substantial contribution of both measurement
585 error (i.e., variation introduced during measurement) and process error (i.e., uncertainty in the
586 actual dynamics that cannot be explained by the deterministic components of the current model)
587 to variation in the data. Estimates of these sources of variation are critical to quantify uncertainty
588 for prediction of ecological dynamics and design sampling efforts (e.g., frequency of sampling
589 within and across years) to maximize the information gained. Explicit inclusion of measurement
590 error (represented by σ in Eq. 7 and 8) and process error (here in both birth rate represented by ϵ
591 and the seasonal pulse represented by Ψ) allowed us to quantify the amount of variation among
592 observations that is attributable to these sources of error. Simulations illustrate that, based on our
593 model, process and measurement variation can lead to a wide range of possible observed values
594 under the conditions of any given year. Although incorporating additional covariates or added

595 realism into the model in future may offer some reduction in the breadth of the simulation
596 intervals, much of this uncertainty may be irreducible given available information. Nevertheless,
597 our results indicate that the data contain important information about predictable changes in the
598 dynamics of the populations, such as the effects of *B. longimanus*, seasonal forcing, and density
599 dependence.

600 The models fit to time series here are relatively simple and yet have provided new
601 insights into interactions among zooplankton in Lake Michigan. Nevertheless, additional realism
602 could likely improve model fit (e.g., better capture the outlier observations in 2011 and 2012)
603 and the strength of inferences gained from the model. For instance, our models only included one
604 prey species, while future models may attempt to incorporate multiple prey species
605 simultaneously and potential interspecific competition or apparent competition mediated by *B.*
606 *longimanus*. Our ability to distinguish between increasingly complex models is limited by
607 available data (i.e., number of observations and years included), although continuing data
608 collection may allow for inference using more complex models. Future work should endeavor to
609 examine the limits to our SSM fitting approach to provide insights under different limitations
610 that are at play in this and many other systems (e.g., sampling frequency, number of data points,
611 levels of measurement error). Additional data collected as a part of the NOAA GLERL Long
612 Term Research program should also provide the opportunity to confirm estimated effects here
613 and test additional drivers of dynamics.

614 Our application of mechanistic models here thus demonstrates how SSMs can provide
615 useful insights into classic questions in ecology, such as the contribution of predators and other
616 drivers to animal population dynamics, which for many systems remains largely hypothetical. In
617 some cases, time series analysis of field data may be the only approach to address such questions
618 at the relevant spatial scale. Fitting of models to data, as we have done here, allows for more
619 direct tests of such fundamental ecological questions in spite of the complex factors involved,
620 including nonlinearities, measurement error, seasonal forcing, and irregular measurement
621 (Bjornstad and Grenfell 2001), which are seldom considered simultaneously. Our findings thus
622 demonstrate the utility of using SSMs and provide a framework for advancing ecological
623 understanding in a mechanistic framework. Further, our results provide novel and valuable
624 example of quantifying NCEs over long timescales at a field scale, providing further evidence
625 for their importance in ecological systems.

626 Finally, the insights gained from testing these hypotheses are vital to understanding and
627 predicting consequences of ongoing large-scale environmental changes, such as the ecosystem-
628 scale shifts caused by invasive species in the Great Lakes. In light of the suite of challenges
629 facing key natural resources globally, advancing understanding of mechanisms for invasive
630 species impacts in the field represents an important step forward.

631

632 **Acknowledgments**

633 We thank Dao Nguyen for assistance with analysis and Craig Stow and Aaron King for
634 helpful discussion. We thank the National Oceanic and Atmospheric Administration Great Lakes
635 Environmental Research Laboratory for sharing data. This work was supported by a National
636 Science Foundation Postdoctoral Research Fellowship in Biology to JAM (DBI-1401837),
637 Michigan DNR funding to JRB, and the Great Lakes Fishery Commission (44066). This is
638 NOAA GLERL Contribution No. 1904 and QFC Publication number 2018-21. SDP
639 acknowledges support from AgBioResearch of Michigan State University. Any use of trade,
640 product, or firm names is for descriptive purposes only and does not imply endorsement by the
641 U.S. Government.

642

643 **Literature Cited**

- 644 Akaike, H. 1974. A new look at the statistical model identification. *IEEE Transactions on*
645 *Automatic Control* 19:716–723.
- 646 Barbiero, R. P., and M. L. Tuchman. 2004. Changes in the crustacean communities of Lakes
647 Michigan, Huron, and Erie following the invasion of the predatory cladoceran
648 *Bythotrephes longimanus*. *Canadian Journal of Fisheries and Aquatic Sciences* 61:2111–
649 2125.
- 650 Beaugrand, G., K. M. Brander, J. A. Lindley, S. Souissi, and P. C. Reid. 2003. Plankton effect on
651 cod recruitment in the North Sea. *Nature* 426:661–664.
- 652 Bjornstad, O., and B. Grenfell. 2001. Noisy clockwork: Time series analysis of population
653 fluctuations in animals. *Science* 293:638–643.
- 654 Bourdeau, P. E., K. L. Pangle, and S. D. Peacor. 2011. The invasive predator *Bythotrephes*
655 induces changes in the vertical distribution of native copepods in Lake Michigan.
656 *Biological Invasions* 13:2533–2545.

- 657 Bourdeau, P. E., K. L. Pangle, and S. D. Peacor. 2015. Factors affecting the vertical distribution
658 of the zooplankton assemblage in Lake Michigan: The role of the invasive predator
659 *Bythotrephes longimanus*. *Journal of Great Lakes Research* 41:115–124.
- 660 Bourdeau, P. E., K. L. Pangle, E. M. Reed, and S. D. Peacor. 2013. Finely tuned response of
661 native prey to an invasive predator in a freshwater system. *Ecology* 94:1449–1455.
- 662 Breto, C., D. H. He, E. L. Ionides, and A. A. King. 2009. Time series analysis in mechanistic
663 models. *Annals of Applied Statistics* 3:319–348.
- 664 Bunnell, D. B., R. P. Barbiero, S. A. Ludsin, C. P. Madenjian, G. J. Warren, D. M. Dolan, T. O.
665 Brenden, R. Briland, O. T. Gorman, J. X. He, T. H. Johengen, B. F. Lantry, B. M. Lesht,
666 T. F. Nalepa, S. C. Riley, C. M. Riseng, T. J. Treska, I. Tsehaye, M. G. Walsh, D. M.
667 Warner, and B. C. Weidel. 2014. Changing ecosystem dynamics in the Laurentian Great
668 Lakes: Bottom-up and top-down regulation. *BioScience* 64:26–39.
- 669 Bunnell, D. B., B. M. Davis, M. A. Chriscinske, K. M. Keeler, and J. G. Mychek-Londer. 2015.
670 Diet shifts by planktivorous and benthivorous fishes in northern Lake Michigan in
671 response to ecosystem changes. *Journal of Great Lakes Research* 41:161–171.
- 672 Bunnell, D. B., B. M. Davis, D. M. Warner, M. A. Chriscinske, and E. F. Roseman. 2011.
673 Planktivory in the changing Lake Huron zooplankton community: *Bythotrephes*
674 consumption exceeds that of *Mysis* and fish. *Freshwater Biology* 56:1281–1296.
- 675 Burnham, K. P., and D. A. Anderson. 2002. *Model Selection and Multimodel Inference: A*
676 *Practical Information-Theoretic Approach*. Springer - Verlag, New York, New York,
677 USA.
- 678 Caceres, C. E. 1998. Interspecific variation in the abundance, production, and emergence of
679 *Daphnia* diapausing eggs. *Ecology* 79:1699–1710.
- 680 Creel, S., J. Winnie, B. Maxwell, K. Hamlin, and M. Creel. 2005. Elk alter habitat selection as an
681 antipredator response to wolves. *Ecology* 86:3387–3397.
- 682 Fahnenstiel, G., T. Nalepa, S. Pothoven, H. Carrick, and D. Scavia. 2010. Lake Michigan lower
683 food web: Long-term observations and *Dreissena* impact. *Journal of Great Lakes*
684 *Research* 36:1–4.
- 685 Heithaus, M. R., A. J. Wirsing, D. Burkholder, J. Thomson, and L. M. Dill. 2009. Towards a
686 predictive framework for predator risk effects: the interaction of landscape features and
687 prey escape tactics. *Journal of Animal Ecology* 78:556–562.

688 Hilborn, R., and M. Mangel. 1997. *The Ecological Detective: Confronting Models with Data*.
689 Princeton University Press, Princeton, New Jersey, USA.

690 Ionides, E. L., C. Breto, and A. A. King. 2006. Inference for nonlinear dynamical systems.
691 PNAS 103:18438–18443.

692 Ionides, E. L., D. Nguyen, Y. Atchade, S. Stoev, and A. A. King. 2015. Inference for dynamic
693 and latent variable models via iterated, perturbed Bayes maps. PNAS 112:719–724.

694 Jacobs, G. R., C. P. Madenjian, D. B. Bunnell, D. M. Warner, and R. M. Claramunt. 2013.
695 Chinook salmon foraging patterns in a changing Lake Michigan. *Transactions of the*
696 *American Fisheries Society* 142:362–372.

697 Keeler, K. M., D. B. Bunnell, J. S. Diana, J. V. Adams, J. G. Mychek-Londer, D. M. Warner, D.
698 L. Yule, and M. R. Vinson. 2015. Evaluating the importance of abiotic and biotic drivers
699 on *Bythotrephes* biomass in Lakes Superior and Michigan. *Journal of Great Lakes*
700 *Research* 41:150–160.

701 Kerfoot, W. C., J. W. Budd, B. J. Eadie, H. A. Vanderploeg, and M. Agy. 2004. Winter storms:
702 Sequential sediment traps record *Daphnia* ephippial production, resuspension, and
703 sediment interactions. *Limnology and Oceanography* 49:1365–1381.

704 Kim, N., and N. D. Yan. 2010. Methods for rearing the invasive zooplankter *Bythotrephes* in the
705 laboratory. *Limnology and Oceanography: Methods* 8:552–561.

706 Kimbro, D. L., J. H. Grabowski, A. R. Hughes, M. F. Piehler, and J. W. White. 2017.
707 Nonconsumptive effects of a predator weaken then rebound over time. *Ecology* 98:656–
708 667.

709 King, A. A., E. L. Ionides, M. Pascual, and M. J. Bouma. 2008. Inapparent infections and
710 cholera dynamics. *Nature* 454:877-U29.

711 King, A. A., D. Nguyen, and E. L. Ionides. 2016. Statistical inference for partially observed
712 Markov processes via the R package pomp. *Journal of Statistical Software* 69.

713 Lehman, J. T., and C. A. Caceres. 1993. Food-web responses to species invasion by a predator
714 invertebrate - *Bythotrephes* in Lake Michigan. *Limnology and Oceanography* 38:879–
715 891.

716 Martinez-Bakker, M., A. A. King, and P. Rohani. 2015. Unraveling the transmission ecology of
717 polio. *PLOS Biology* 13.

718 Matassa, C. M., and G. C. Trussell. 2011. Landscape of fear influences the relative importance of
719 consumptive and nonconsumptive predator effects. *Ecology* 92:2258–2266.

720 Nelson, E. H., C. E. Matthews, and J. A. Rosenheim. 2004. Predators reduce prey population
721 growth by inducing changes in prey behavior. *Ecology* 85:1853–1858.

722 Newman, K., S. T. Buckland, B. Morgan, R. King, D. L. Borchers, D. Cole, P. Besbeas, O.
723 Gimenez, and L. Thomas. 2014. *Modelling Population Dynamics: Model Formulation,*
724 *Fitting and Assessment using State-Space Methods.* Springer-Verlag, New York, New
725 York, USA.

726 Nowicki, C. J., D. B. Bunnell, P. M. Armenio, D. M. Warner, H. A. Vanderploeg, J. F.
727 Cavaletto, C. M. Mayer, and J. V. Adams. 2017. Biotic and abiotic factors influencing
728 zooplankton vertical distribution in Lake Huron. *Journal of Great Lakes Research*
729 43:1044–1054.

730 Pangle, K. L., and S. D. Peacor. 2006. Non-lethal effect of the invasive predator *Bythotrephes*
731 *longimanus* on *Daphnia mendotae*. *Freshwater Biology* 51:1070–1078.

732 Pangle, K. L., and S. D. Peacor. 2009. Light-dependent predation by the invertebrate planktivore
733 *Bythotrephes longimanus*. *Canadian Journal of Fisheries and Aquatic Sciences* 66:1748–
734 1757.

735 Pangle, K. L., S. D. Peacor, and O. E. Johannsson. 2007. Large nonlethal effects of an invasive
736 invertebrate predator on zooplankton population growth rate. *Ecology* 88:402–412.

737 Panik, M. J. 2017. *Stochastic Population Growth Models.* Pages 167–191 *Stochastic Differential*
738 *Equations.* John Wiley & Sons, Inc., Hoboken, New Jersey, USA.

739 Peckarsky, B. L., P. A. Abrams, D. I. Bolnick, L. M. Dill, J. H. Grabowski, B. Luttbeg, J. L.
740 Orrock, S. D. Peacor, E. L. Preisser, O. J. Schmitz, and G. C. Trussell. 2008. Revisiting
741 the classics: Considering nonconsumptive effects in textbook examples of predator-prey
742 interactions. *Ecology* 89:2416–2425.

743 van de Pol, M., L. D. Bailey, N. McLean, L. Rijdsdijk, C. R. Lawson, and L. Brouwer. 2016.
744 Identifying the best climatic predictors in ecology and evolution. *Methods in Ecology and*
745 *Evolution* 7:1246–1257.

746 R Core Team. 2018. *R: A Language and Environment for Statistical Computing.* R Foundation
747 for Statistical Computing, Vienna, Austria.

748 Scheffer, M., D. Straile, E. H. van Nes, and H. Houser. 2001. Climatic warming causes regime
749 shifts in lake food webs. *Limnology and Oceanography* 46:1780–1783.

750 Turchin, P., and A. Taylor. 1992. Complex dynamics in ecological time-series. *Ecology* 73:289–
751 305.

752 Vanderploeg, H. A., S. A. Pothoven, G. L. Fahnenstiel, J. F. Cavaletto, J. R. Liebig, C. A. Stow,
753 T. F. Nalepa, C. P. Madenjian, and D. B. Bunnell. 2012. Seasonal zooplankton dynamics
754 in Lake Michigan: Disentangling impacts of resource limitation, ecosystem engineering,
755 and predation during a critical ecosystem transition. *Journal of Great Lakes Research*
756 38:336–352.

757 Vanderploeg, H., J. Liebig, and M. Omair. 1993. *Bythotrephes* predation on Great Lakes
758 zooplankton measured by an in situ method - Implications for zooplankton community
759 structure. *Archiv Fur Hydrobiologie* 127:1–8.

760 Yurista, P. M., H. A. Vanderploeg, J. R. Liebig, and J. F. Cavaletto. 2010. Lake Michigan
761 *Bythotrephes* prey consumption estimates for 1994–2003 using a temperature and size
762 corrected bioenergetic model. *Journal of Great Lakes Research* 36:74–82.

764 DATA AVAILABILITY

765 Data are available from the Dryad Digital Repository: <https://doi.org/10.5061/dryad.bh688ft>

766 **Table 1:** Model Δ AIC values relative to best model (lowest AIC).

Model	Maximum Log-Likelihood	Parameters	AIC	Δ AIC
a. No <i>B. longimanus</i> effect	-213.3	11	448.6	6.9
b. <i>B. longimanus</i> nonconsumptive effect	-208.9	12	441.7	0.0
c. <i>B. longimanus</i> consumption	-212.5	12	449.1	7.3
d. Consumption and nonconsumptive effect	-208.7	13	443.4	1.7
e Monthly average I.I.D.	-336.3	13	698.5	256.8
f. AR (2) with measurement error	-369.4	6	750.7	309.0
g. <i>Limnocalanus</i> nonconsumptive effect	-212.5	12	449.1	7.3
h. <i>B. longimanus</i> anomaly	-210.2	12	444.4	2.6

i. Seasonal birth and background death	-210.4	14	448.9	7.2
j. Seasonal birth and attack rate	-210.1	15	450.3	8.5
k. Type II functional response	-212.0	13	450.0	8.9

767

768 **Table 2:** Values of model terms at maximum likelihood estimate for best fit model (b).

Parameter	Description	Estimate	Units
λ_1	Seasonal birth rate	-10.0	$\ln(\text{day}^{-1})$
λ_2	Seasonal birth rate	-3.4	$\ln(\text{day}^{-1})$
λ_3	Seasonal birth rate	-1.2	$\ln(\text{day}^{-1})$
λ_4	Seasonal birth rate	0.32	$\ln(\text{day}^{-1})$
κ	Density dependence term	32.5	$\text{mg} \times \text{m}^{-3}$
μ	Background mortality	0.048	day^{-1}
α	Attack rate	NA	$(\text{mg } B. \text{ longimanus})^{-1} \times \text{day}^{-1}$
η	Induced proportional birth reduction	0.089	$(\ln(\text{mg } B. \text{ longimanus}))^{-1}$
ϵ	Standard deviation of growth rate	0.26	day^{-1}
φ	$\ln(\text{Spring pulse mean})$	-3.2	$\text{mg} \times \text{m}^{-3}$
Ψ	Standard deviation of $\ln(\text{Spring pulse})$	1.7	$\text{mg} \times \text{m}^{-3}$
σ_a	Measurement error (scales with $V_{(T)}$)	0.22	$\text{mg} \times \text{m}^{-3}$
σ_b	Measurement error (scales with $V_{(T)}^2$)	0.39	$\text{mg} \times \text{m}^{-3}$

769

770

Figure Legends

771 **Figure 1:** Simulated *Daphnia mendotae* biomass density (mg/m^3) from fitted model compared to772 *D. mendotae* and *Bythotrephes longimanus* time series data in Lake Michigan from 1994-2012.

773 Median and 95% simulation intervals for the model that only includes nonconsumptive effects

774 (model b); Black solid line: *D. mendotae*; Red dashed line: *B. longimanus*; blue dashed line:775 median simulated *D. mendotae* biomass density; dark blue dotted line: 95% simulation intervals.776 The first observations in 2007 and 2012 and the *D. mendotae* peak in 2011 are cut off from the

777 plot.

778

779 **Figure 2:** For the fitted model (model b, which only includes nonconsumptive effects): a)

780 estimated seasonal birth rate and b) simulated biomass density (from 10,000 simulations) of

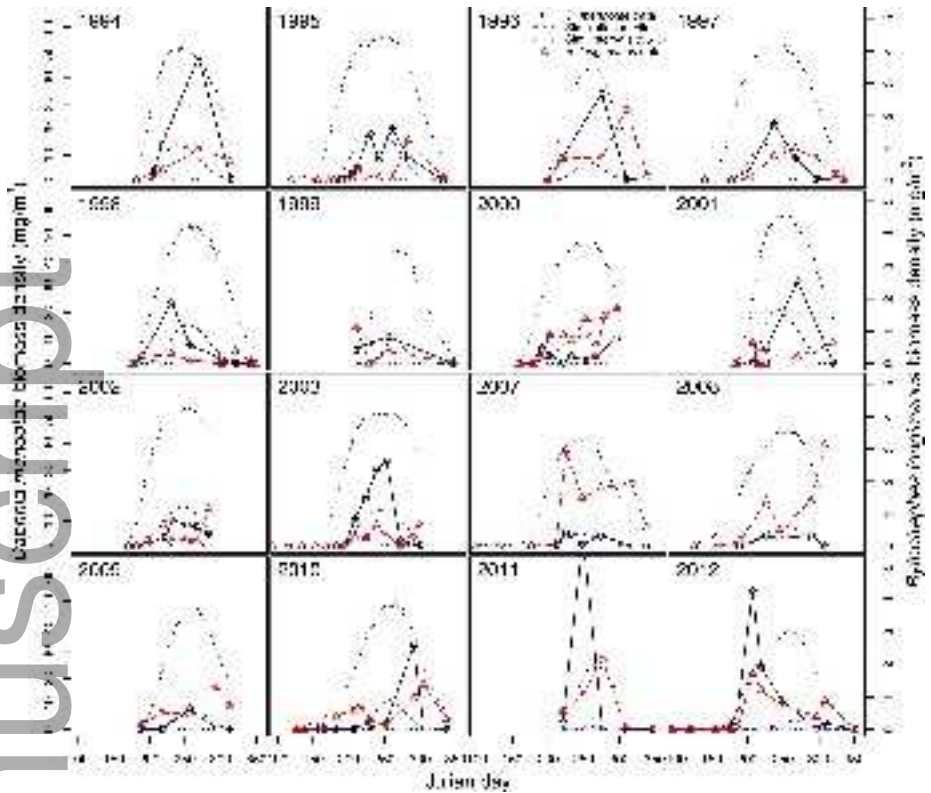
781 *Daphnia mendotae* in the presence (green dashed line) or absence (black solid line) of
782 *Bythotrephes longimanus*. Growth rates and simulated density were determined using across-
783 year averages of smoothed *B. longimanus* biomass density (red dashed line in plot b) for each
784 Julian day. Estimated background mortality rate is indicated by the blue dotted line in (a).

785

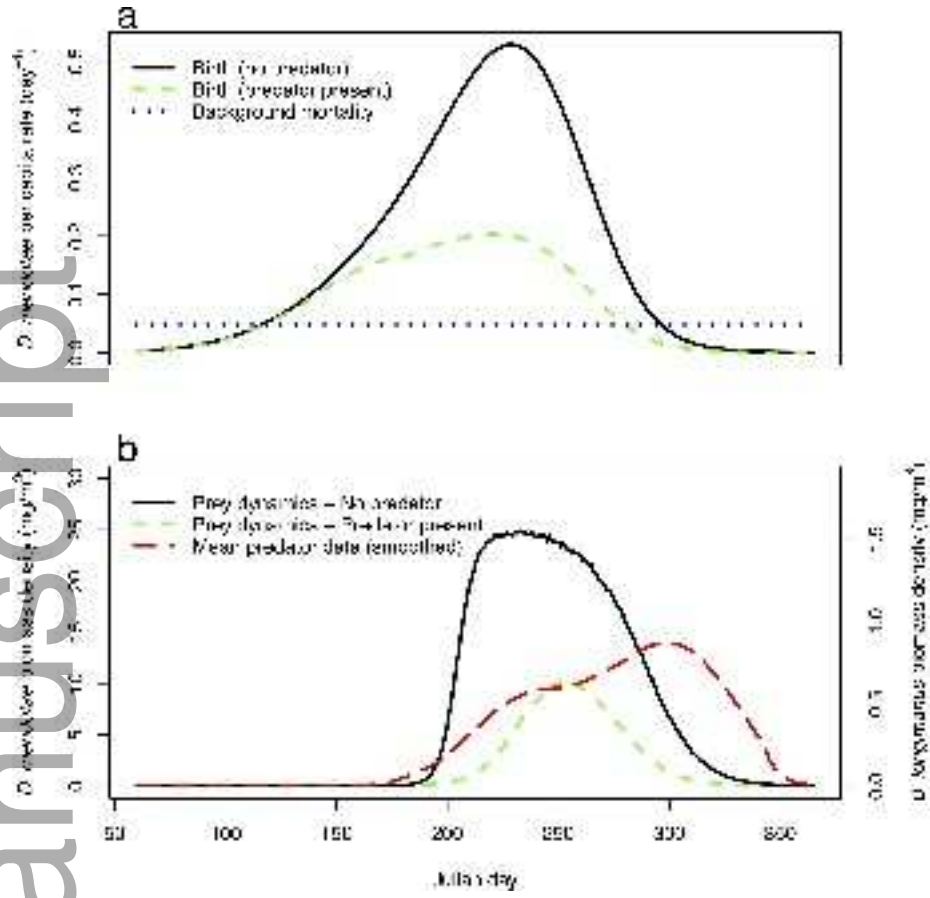
786 **Figure 3:** Likelihood profiles for a) η (reduction in *Daphnia mendotae* birth rate in response to
787 *Bythotrephes longimanus*) and b) κ (density dependence) parameters. Black vertical lines
788 indicate 95% confidence intervals (η : 0.038-0.11 $(\ln(\text{mg } B. longimanus))^{-1}$; κ : 22.5-55.6 mg *D.*
789 *mendotae* per m^3). Black points show the two highest maximum likelihood estimates from the
790 searches performed at each parameter value for each profile, blue lines show a loess smoothed
791 curve fit to those points, and gray shading (approximately the width of the points) indicates
792 confidence intervals for the loess fit.

793

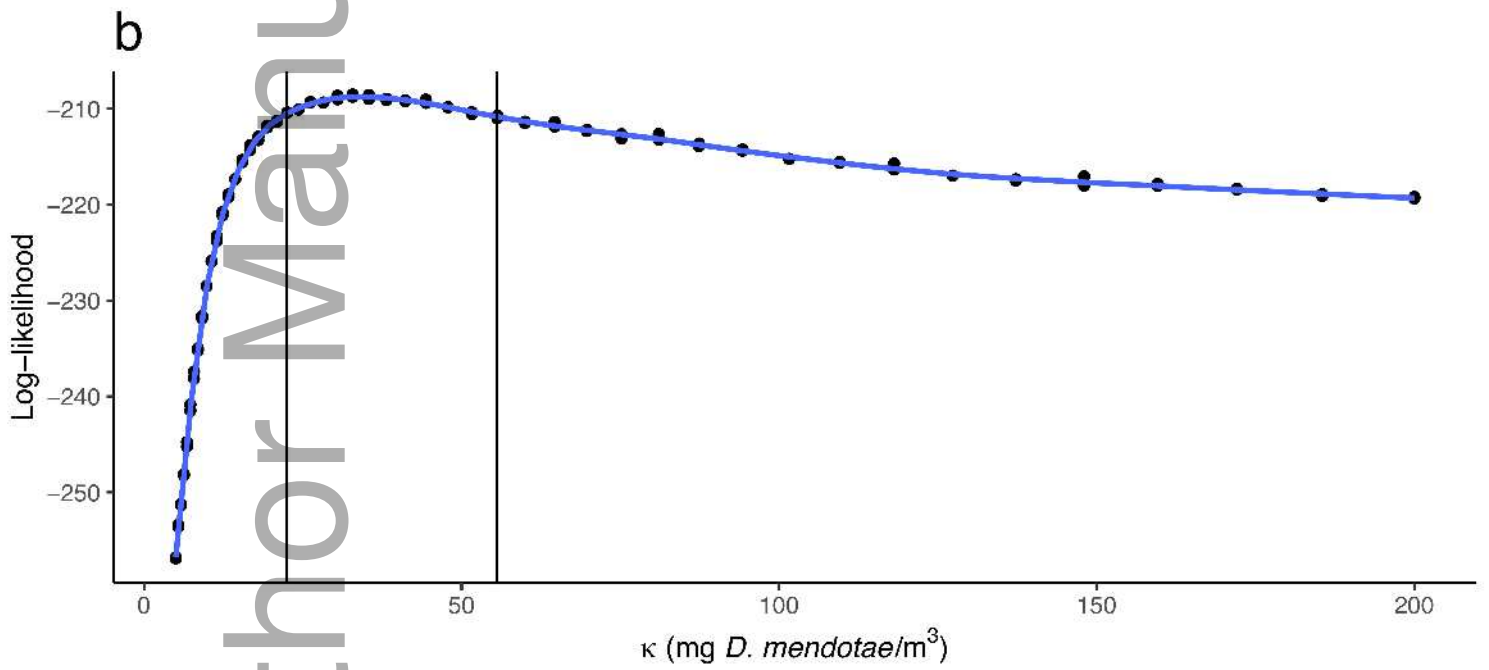
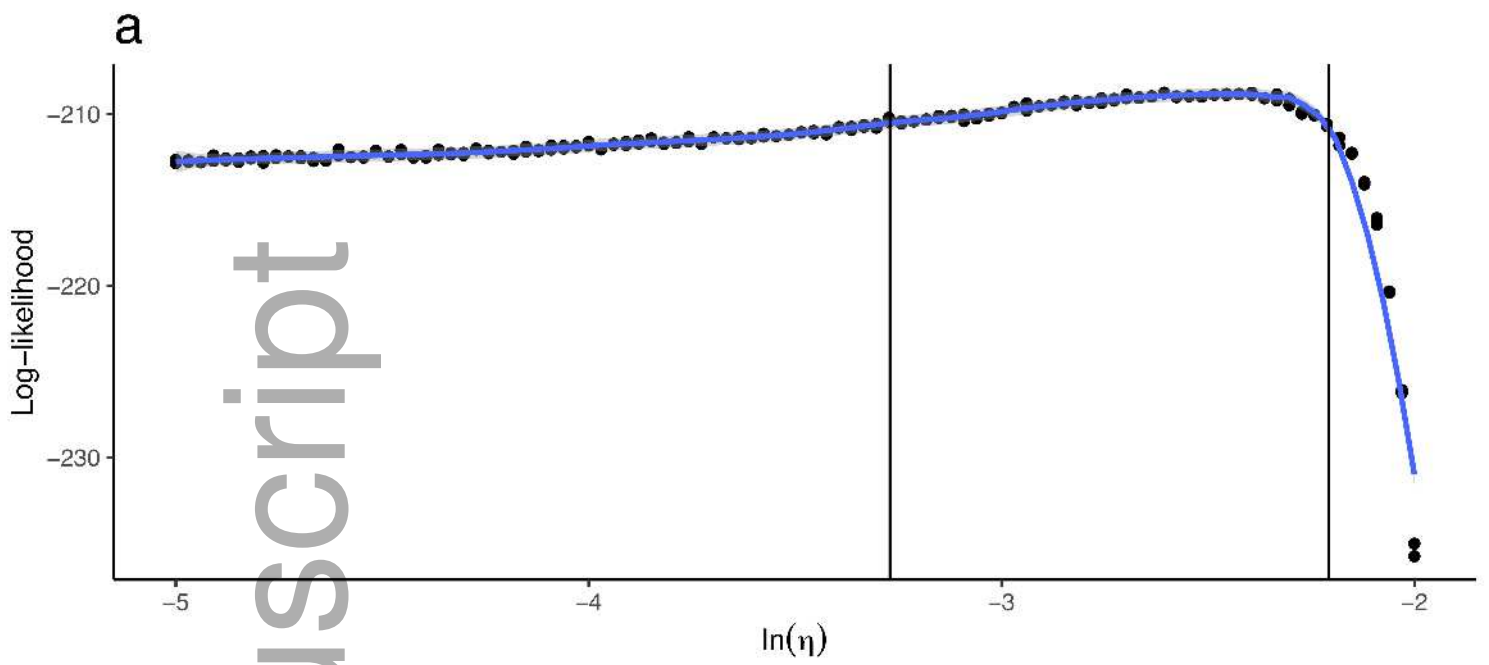
794 **Figure 4:** Estimated rate of change in *Daphnia mendotae* population early in growing season
795 (days 175-225, calculated via Eq. 12) vs. smoothed *Bythotrephes longimanus* biomass density
796 (geometric mean of smoothed *B. longimanus* + 0.005 over days 175-225) each year. Points are
797 shown as 2-digit numbers representing each year.



ecy_2583_f1.jpg

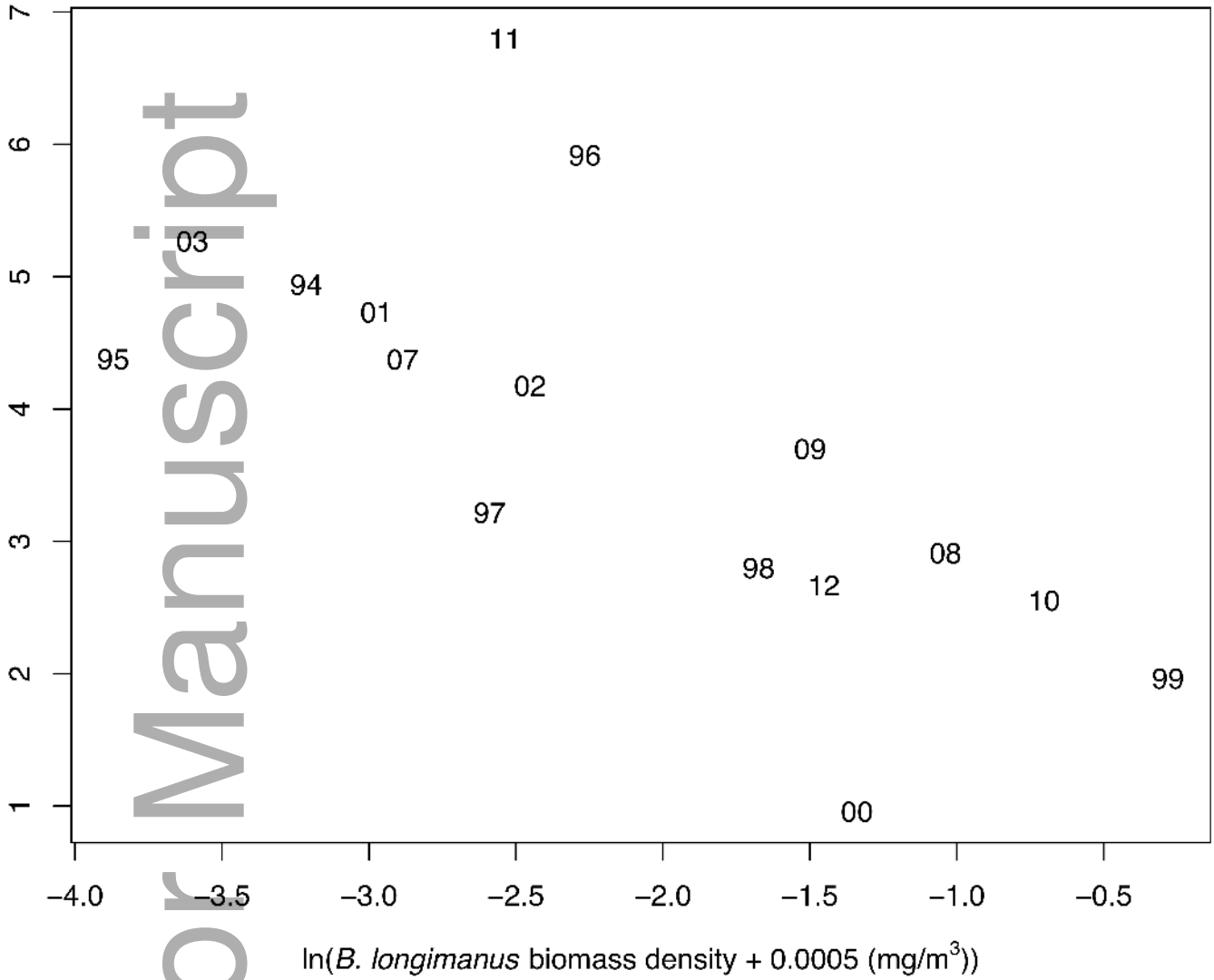


ecy_2583_f2.jpg



ecy_2583_f3.jpg

D. mendotae estimated rate of population change (days 175–225)



ecy_2583_f4.jpg